ChemComm

An Ester Electrolyte for Lithium–Sulfur Batteries Capable of Ultra-Low Temperature Cycling

Journal:	*ChemComm*
Manuscript ID	CC-COM-05-2020-003798.R1
Article Type:	Communication

COMMUNICATION

An Ester Electrolyte for Lithium–Sulfur Batteries Capable of Ultra-Low Temperature Cycling

Received 00th January 20xx,
Accepted 00th January 20xx

DOI: 10.1039/x0xx00000x

Guorui Cai,[a] John Holoubek,[a] Dawei Xia,[a] Mingqian Li,[c] Yijie Yin,[b] Xing Xing,[b] Ping Liu[a,b,c,d] and Zheng Chen*[a,b,c,d]

A novel lithium bis(fluorosulfonyl)imide in methyl propionate/ fluoroethylene carbonate (LiFSI MP/FEC) electrolyte was designed for high compatibility with Li metal and sulfurized polyacrylonitrile (SPAN). The resulted Li||SPAN cells can charge and discharge at -20 °C and -40 °C with over 91% and 78% room temperature capacity retention.

The demand for rechargeable batteries with increased energy density at sub-zero temperatures is increasing, especially for portable devices in harsh environments such as high altitude, arctic regions, outer space, and abyss explorations.[1-3] However, state-of-the-art Li-ion batteries (LIBs) comprised of a graphite anode (372 mAh g^{-1}) and a lithium transition metal oxide cathode cannot conceivably deliver > 300 Wh kg^{-1} at the cell level, which deteriorates even further at extremely cold conditions.[4,5]

To raise the energy density of LIBs, a large amount of effort has been focused on the employment of Li metal (3860 mAh g^{-1}), the highest-energy-density anode.[6,7] Additionally, abundantly available elemental sulfur, with a theoretical energy density of 2600 Wh kg^{-1}, has also received attention as a next-generation cathode material.[8,9] Unfortunately, Li-S batteries encounter limitations such as the low utilization of active materials and poor cycling performance, which is caused by the electronically insulating nature of sulfur, shuttling of soluble polysulfide intermediates, and the instability of the Li anode. As an alternative solution, Li-S batteries based on sulfur composites, such as sulfurized polyacrylonitrile (SPAN),[10-16] have been shown to effectively overcome some of the problems associated with sulfur electrodes. Despite the high compatibility of SPAN with carbonate-based electrolytes, practical cells typically fail to achieve stable long-term cycling due to the poor Li metal stability found in such electrolytes.[10-16]

Furthermore, the high melting point of carbonate electrolytes further limits the application of Li-SPAN batteries at low temperatures. To preserve energy output, numerous reports have been focused on the development of low-temperature electrolytes to increase ionic conductivity and reduce charge transfer resistance in current LIBs.[17-26] Carboxylate ester-based co-solvents with low melting points and viscosity are commonly employed to do so.[21-25] However, these molecules are of high reactivity with Li metal, resulting in reduced cycling performance and hazardous dendrite growth, especially at extremely cold temperatures.[27] To improve the performance of such carboxylate ester-containing electrolytes, fluoride-donating additives have been introduced in previous works for the production of fluorine-rich solid electrolyte interphase (SEI) layers to improve the cycling performance of the Li metal anode, which simultaneously provided the Li metal anode with improved reversibility and sub-zero temperature performance.[23-25] However, to the best our knowledge, electrolytes that simultaneously enable lithium metal and sulfur-based cathodes at extremely low-temperature remain a significant challenge.

Herein, a new ester-based electrolyte is developed for Li-SPAN batteries capable of cycling at ultra-low temperatures, in which methyl propionate (MP), a common carboxylate ester with a low melting point (-87.5 °C) and suitable dielectric constant (6.23), is used as the primary solvent. Fluoroethylene carbonate (FEC, 10% by volume) and Lithium bis(fluorosulfonyl)imide (LiFSI, 1M) are applied as a co-solvent additive and the Li salt, respectively, both of which which are known to stabilize the SEI. [10,12,13, 23-26] As a result, this LiFSI MP/FEC electrolyte system exhibited high compatibility with both the Li metal anode and SPAN cathode, and thus provided the high room temperature capacity retention (> 78%) and cycling stability (capacity fade < 0.14% per cycle) even at -40 °C.

[a] Department of NanoEngineering, University of California, San Diego, La Jolla, CA 92093, USA.
E-mail: zhengchen@eng.ucsd.edu; Web: http://zhengchen.eng.ucsd.edu/
[b] Program of Materials Science, University of California, San Diego, La Jolla, CA 92093, USA
[c] Program of Chemical Engineering, University of California, San Diego, La Jolla, CA 92093, USA
[d] Sustainable Power and Energy Center, University of California, San Diego, La Jolla, CA 92093, USA

† Electronic Supplementary Information (ESI) available: Materials synthesis and fabrication, supplemental figures. See DOI: 10.1039/x0xx00000x

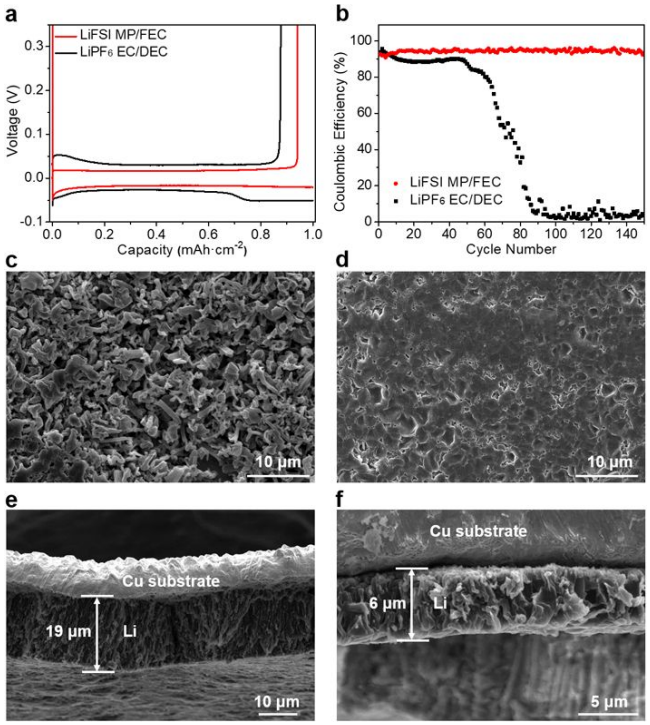

Fig. 1 Li metal performance in selected electrolytes at room temperature. (a) Li plating/stripping curves and (b) long-term cycling performance of Li||Cu cells in LiFSI MP/FEC, and $LiPF_6$ EC/DEC at 0.5 mA cm^{-2}; Top (c and d) and cross-section (e and f) views of SEM images of Li deposit obtained in $LiPF_6$ EC/DEC (c and e), and LiFSI MP/FEC (d and f) at 1 mAh cm^{-2} and 0.5 mA cm^{-2}.

In order to investigate the compatibility of the LiFSI MP/FEC electrolyte with the Li metal anode, Li||Cu cells with different electrolytes were assembled. The industry-type 1M $LiPF_6$ in ethylene carbonate/diethyl carbonate (EC/DEC, 1:1 in volume) electrolyte was selected as the control electrolyte due to a large volume of published work conducted with similar formulations in this research field.[10-15] As is shown in Fig. 1a, the LiFSI MP/FEC electrolyte provides smooth plating/stripping curves with a significantly higher Coulombic efficiency (CE) than the $LiPF_6$ EC/DEC system (94.2% *vs.* 88.3%), indicating that the former exhibits higher compatibility with the Li metal anode. This trend is further supported by the long-term cycling performance (Fig. 1b), in which LiFSI MP/FEC retains a CE of 93.4% after 150 cycles. In contrast, the CE of the industry-type electrolyte system suffered a vast drop after 50 cycles, as a result of the continuous formation of porous inactive Li and depletion of electrolyte.[28-30] To further compare their Li plating behavior, Li||Cu cells after plating 1 mAh cm^{-2} of Li at 0.5 mA cm^{-2} were disassembled and the morphology of plated Li was examined by scanning electron microscopy (SEM), in which the $LiPF_6$ EC/DEC system produced a highly dendritic Li structure (Fig. 1c), a common phenomenon for similar electrolyte systems with poor reductive stability towards Li metal.[24,27,28] The LiFSI MP/FEC electrolyte system, on the other hand exhibited large Li chunks without noticeable dendrites (Fig. 1d). Based on SEM images of the cross-section (Fig. 1e and f), the plated Li in $LiPF_6$ EC/DEC electrolyte exhibited a thickness of ~ 19 μm, whereas the plated Li in LiFSI MP/FEC electrolyte presented a dense structure with a thickness of ~ 6 μm, close to the calculated theoretical thickness of 4.8 μm, which indicates a low porosity (~ 20%) , and thus minimizes the Li surface area and its parasitic reactions with the electrolyte.[28-30] Therefore, all the above results indicate the superiority of the LiFSI MP/FEC system for Li metal anode stability.

To test the effect of these electrolytes on the performance of the SPAN cathode, Li||SPAN half cells were assembled. As observed in Fig. 2a and b, the LiFSI MP/FEC system provides typical charge-discharge curves commonly found in carboxylate ester-based electrolyte systems.[10-15] In addition, long-term cycling tests demonstrated LiFSI MP/FEC system with a capacity retention of 81% after 100 cycles, as well as a CE of ~ 99.9% at 0.5 A g^{-1}, indicating SPAN has negligible dissolution and shuttling in the LiFSI MP/FEC system (Fig. 2b and S1, ESI†).[25]

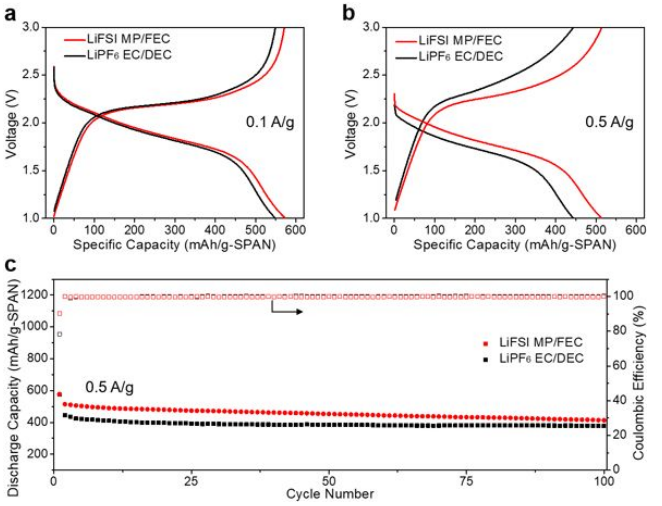

Fig. 2 Li||SPAN half-cell performance in different electrolytes at room temperature. Voltage curves at (a) 0.1 A g^{-1} and (b) 0.5 A g^{-1}; (c) Long-term cycling performance at 0.5 A g^{-1}.

To demonstrate the advantage of LiFSI MP/FEC electrolyte at sub-zero temperature, after activation at room temperature for two cycles, Li||SPAN half cells were cycled at -20 and -40 °C. The corresponding voltage profiles at 0.1 A g^{-1} are displayed in Fig. 3a and b. While both electrolyte systems show comparable capacity and cycling stability at room temperature (Fig. 2a, and c), the capacity retention of these cells with the industry-type carbonate electrolyte suffers a dramatic fade of both operating voltage and capacity with the decrease of testing temperature. Especially at -40 °C (Fig. 3b), the $LiPF_6$ EC/DEC electrolyte system retained less than 1% of its room temperature capacity, a result similar in our previous works, attributed to a strong binding between Li^+ and EC, as well as a high melting point of EC/DEC solvent.[24] On the contrary, the LiFSI MP/FEC electrolyte system is superior in the above respects, in which the low melting point of MP ensures the high retention of ionic conductivity at extremely cold temperature, and the replacement of EC with FEC allows for a facile de-solvation process due to the significantly weaker Li^+ binding energy of FEC.[24] As a result, the MP/FEC system was able to offer a 91% and 78% room-temperature capacity retention at 0.1 A g^{-1} and -20 °C and -40 °C, respectively (Fig. 2a, 3a, and 3b). To further highlight their ability to work at ultra-low temperatures, the long-term cycling of Li-SPAN half cells was conducted at -20 and -40 °C (Fig. 3c and

S2, ESI †), where over 86% capacity of initial capacity was maintained for 100 cycles at 0.2 A g^{-1}.

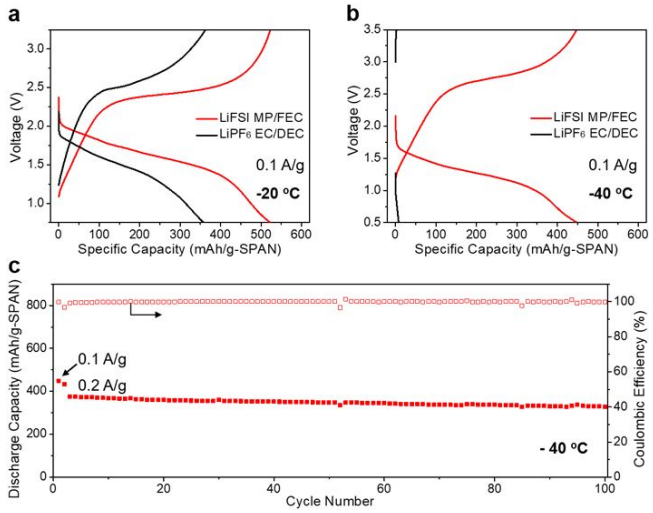

Fig. 3 Li||SPAN half cells performance at ultra-low temperature. Voltage curves of Li||SPAN cells at (a) -20 °C, and (b) -40 °C with a current density of 0.1 A g^{-1} in each electrolyte; (c) Long-term cycling performance of Li||SPAN half cells charging and discharging at -40 °C in LiFSI MP/FEC.

To better understand the performance of these Li||SPAN cells at extremely low temperatures, further electrochemical characterization was performed. Electrochemical impedance spectroscopy (EIS) of 50% state of charge (SOC) symmetric positive electrode cells was applied in addition to EIS of Li||Li and Li||SPAN cells to deconvolute the respective impedance contributions.[23] It was observed that the Li||SPAN cells exhibited charge transfer impedances of 75, 1140, and 7762 Ω at 25, -20, and -40 °C, respectively, far beyond the bulk ionic resistance (~ 3, 6, and 12 Ω). In order to probe the anode and cathode sides, symmetric Li||Li cell and SPAN||SPAN cell at 50% SOC were analysed under the same conditions (Fig. 4a-c). Although both anode and cathode sides exhibited a small charge transfer impedance at room temperature (16 and 55 Ω), the Li metal side provides consistently higher impedance than the SPAN cathode at sub-zero temperatures, producing charge transfer impedances of 2126, and 15470 Ω compared to only 737, and 5280 Ω at -20, and -40 °C, respectively. This resistance trend for the Li anode was also investigated in Li||Cu cells at 0.15 mA cm^{-2}. As shown in Fig. 4d, the Li||Cu cells provide a ~ 0.007 V, 0.25 V, and 0.60 V overpotential at room temperature, -20 °C and -40 °C, respectively. Their increased overpotentials at low temperatures (-20 °C and -40 °C) in comparison with those at room temperature share the same trend as those with the Li||SPAN half cells (~ 0.24 V and 0.59 V *vs.* ~ 0.26 V and 0.61 V), indicating that the rapidly increased impedance on anode side is the main reason responsible for reduced capacity of Li||SPAN half cells at ultra-low temperatures. Corresponding data in the $LiPF_6$ EC/DEC (Fig. S3-S5, ESI†) electrolyte system also exhibited the same trend as the above results, but this electrolyte system showed a ~ 300% higher impedance at ultralow temperatures, which is consistent with the significantly lower capacity retention under these conditions (Fig. 3a and b).

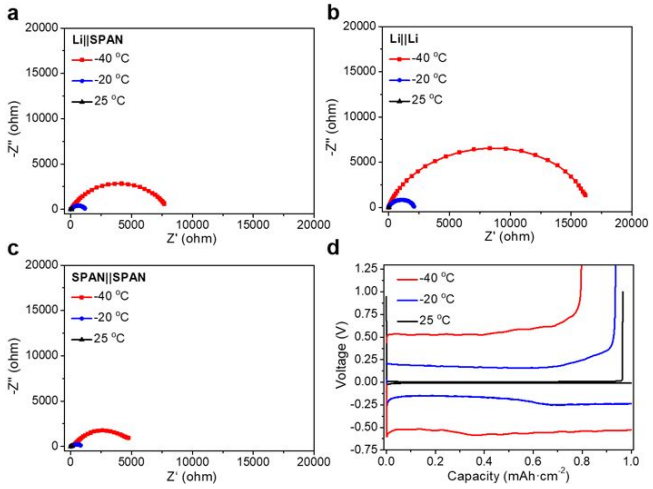

Fig. 4 Electrochemical behavior of selected electrolytes in Li||SPAN half cells, Li||Li and SPAN||SPAN symmetrical cells at different temperatures. Nyquist plots of (a) Li||SPAN half cells, (b) Li||Li symmetrical cells, and (c) SPAN||SPAN cells at 25 °C, -20 °C, and -40 °C in LiFSI MP/FEC; (d) Voltage curves of Li||Cu cells at 25 °C, -20 °C, and -40 °C in LiFSI MP/FEC at 0.15 mA cm^{-2} and 1 mAh cm^{-2}.

In summary, a carboxylate ester-based electrolyte system for ultra-low temperature Li-SPAN batteries was developed, in which the main solvent MP ensures a low melting point, and the fluoride-donating FSI and FEC components improve the compatibility of MP with Li metal. Electrochemical results show that such LiFSI MP/FEC electrolyte can provide Li||SPAN cells with higher Li metal compatibility (CE: 94.2% vs. 88.3% at room temperature) and long-term stability than the industry-type carbonate electrolyte at room and ultra-low temperature due to the improved compatibility with both Li metal anodes and SPAN cathodes. When cycled at a current density of 0.1 A g^{-1}, Li||SPAN half cells retained over 91% and 78% of their room temperature capacity at -20 °C and -40 °C, respectively. The Li-SPAN cells also retained 86% of their initial capacity at 0.2 A g^{-1} after 100 cycles at -40 °C. Different from strategies attempted to preserve energy output of LIBs,[3,24,31,32] this work provides crucial design strategy for rechargeable batteries with high energy density at ultra-low temperature through simultaneously increasing the baseline energy density of the battery and lower the energy loss at sub-zero temperatures.

This work was partially supported by an Early Career Faculty grant from NASA's Space Technology Research Grants Program (ECF 80NSSC18K1512). Z.C. also acknowledges the start-up fund from Jacob School of Engineering at UCSD. The majority of cell fabrication and electrochemical testing was performed in the UCSD-MTI Battery Fabrication and the UCSD-Arbin Battery Testing Facility. This work was performed in part at the San Diego Nanotechnology Infrastructure (SDNI) of UCSD, a member of the National Nanotechnology Coordinated Infrastructure, which is supported by the National Science Foundation (Grant ECCS-1542148).

Conflicts of interest

There are no conflicts to declare.

Notes and references

1 M. C. Smart, B. V. Ratnakumar, R. C. Ewell, S. Surampudi, F. J. Puglia and R. Gitzendanner, *Electrochim. Acta*, 2018, **268**, 27-40.
2 K. B. Chin, E. J. Brandon, R. V. Bugga, M. C. Smart, S. C. Jones, F. C. Krause, W. C. West and G. G. Bolotin, *Proc. IEEE*, 2018, **106**, 419-428.
3 M.-T. F. Rodrigues, G. Babu, H. Gullapalli, K. Kalaga, F. N. Sayed, K. Kato, J. Joyner and P. M. Ajayan, *Nat. Energy*, 2017, **2**, 17108.
4 J. Jaguemont, L. Boulon and Y. Dubé, *Appl. Energy*, 2016, **164**, 99-114.
5 C. K. Huang, J. S. Sakamoto, J. Wolfenstine and S. Surampudi, *J. Electrochem. Soc.*, 2000, **147**, 2893-2896.
6 J. Liu, Z. Bao, Y. Cui, E. J. Dufek, J. B. Goodenough, P. Khalifah, Q. Li, B. Y. Liaw, P. Liu, A. Manthiram, et al., *Nat Energy*, 2019, **4**, 180-186.
7 X. Fan, L. Chen, O. Borodin, X. Ji, J. Chen, S. Hou, T. Deng, J. Zheng, C. Yang, S.-C. Liou, et al., *Nat. Nanotechnol.*, 2018, **13**, 715-722.
8 Q. Pang, X. Liang, C. Y. Kwok and L. F. Nazar, *Nat. Energy*, 2016, **1**, 16132.
9 A. Gupta, A. Bhargav, J. P. Jones, R. V. Bugga and A. Manthiram, *Chem. Mater.*, 2020, **32**, 2070-2077.
10 H. Yang, J. Chen, J. Yang and J. Wang, *Angew. Chem., Int. Ed.*, 2020, **59**, 7306-7318.
11 J. Wang, Y. S. He and J. Yang, *Adv. Mater.*, 2015, **27**, 569-575.
12 W.-J. Chen, B.-Q. Li, C.-X. Zhao, M. Zhao, T.-Q. Yuan, R.-C. Sun, J.-Q. Huang and Q. Zhang, *Angew. Chem., Int. Ed.*, 2019, https://doi.org/10.1002/anie.201912701.
13 Z. Chen, J. Zhou, Y. Guo, C. Liang, J. Yang, J. Wang and Y. Nuli, *Electrochim. Acta*, 2018, **282**, 555-562.
14 Z. Xu, J. Wang, J. Yang, X. Miao, R. Chen, J. Qian and R. Miao, *Angew. Chem., Int. Ed.*, 2016, **55**, 10372-10375.
15 S. Wei, L, Ma, K. E. Hendrickson, Z. Tu and L. A. Archer. *J. Am. Chem. Soc.*, 2015, **137**, 12143-12152.
16 X. Xing, Y. Li, X. Wang, V. Petrova, H. Liu and P. Liu, *Energy Storage Mater.*, 2019, **21**, 474-480.
17 C. S. Rustomji, Y. Yang, T. K. Kim, J. Mac, Y. J. Kim, E. Caldwell, H. Chung and Y. S. Meng, *Science*, 2017, **356**, eaal4263.
18 X. Fan, X. Ji, L. Chen, J. Chen, T. Deng, F. Han, J. Yue, N. Piao, R. Wang, X. Zhou, *et al.*, *Nat. Energy*, 2019, **4**, 882-890.
19 Q. Li, S. Jiao, L. Luo, M. S. Ding, J. Zheng, S. S. Cartmell, C.-M. Wang, K. Xu, J.-G. Zhang and W. Xu, *ACS Appl. Mater. Interfaces* 2017, **9**, 18826-18835.
20 S. S. Zhang, K. Xu, J. L. Allen and T. R. Jow, *J. Power Sources*, 2002, **110**, 216-221.
21 M. C. Smart, B. V. Ratnakumar, K. B. Chin and L. D. Whitcanack, *J. Electrochem. Soc.*, 2010, **157**, A1361-A1374.
22 X. Dong, Z. Guo, Z. Guo, Y. Wang and Y. Xia, *Joule*, 2018, **2**, 902-913.
23 J. Holoubek, Y. J. Yin, M.Q. Li, M.Y. Yu, Y.M. Meng, P. Liu and Z. Chen, *Angew. Chem., Int. Ed.*, 2019, **58**, 18892-18897.
24 J. Holoubek, M. Yu, S. Yu, M. Li, Z. Wu, D. Xia, P. Bhaladhare, M.S. Gonzalez, T. A. Pascal, P. Liu and Z. Chen, *ACS Energy Lett.*, 2020, **5**, 1438-1447.
25 M. C. Smart, B. L. Lucht, S. Dalavi, F. C. Krause and B. V. Ratnakumar, *J. Electrochem. Soc.*, 2012, **159**, A739-A751.
26 E. Markevich, G. Salitra and D. Aurbach, *ACS Energy Lett.*, 2017, **2**, 1337-1345.
27 A. C. Thenuwara, P. P. Shetty and M. T. McDowell, *Nano Lett.*, 2019, **19**, 8664-8672.
28 S. Chen, J. Zheng, D. Mei, K. S. Han, M. H. Engelhard, W. Zhao, W. Xu, J. Liu and J.-G. Zhang, *Adv. Mater.*, 2018, **30**, 1706102.
29 S. Li, M. Jiang, Y. Xie, H. Xu, J. Jia and J. Li, *Adv. Mater.*, 2018, **30**, 1706375.
30 C. Fang, J. Li, M. Zhang, Y. Zhang, F. Yang, J. Z. Lee, M.-H. Lee, J. Alvarado, M. A. Schroeder, Y. Yang, B. Lu, N. Williams, M. Ceja, L. Yang, M. Cai, J. Gu, K. Xu, X. Wang and Y. S. Meng, *Nature*, 2019, **572**, 511-515.
31 C.-Y. Wang, G. Zhang, S. Ge, T. Xu, Y. Ji, X.-G. Yang and Y. Leng, *Nature*, 2016, **529**, 515-518.
32 B. Liao, H. Li, M. Xu, L. Xing, Y. Liao, X. Ren, W. Fan, L. Yu, K. Xu and W. Li, *Adv. Energy Mater.*, 2018, **8**, 1800802.